



Functional annotation and characterization of 3-hydroxybenzoate 6-hydroxylase from *Rhodococcus jostii* RHA1

Stefania Montersino, Willem J.H. van Berkel *

Laboratory of Biochemistry, Wageningen University, Dreijenlaan 3, 6703 HA Wageningen, The Netherlands

ARTICLE INFO

Article history:

Received 7 October 2011

Received in revised form 9 December 2011

Accepted 14 December 2011

Available online 22 December 2011

Keywords:

Fingerprint

Flavoprotein

Functional annotation

3-hydroxybenzoate 6-hydroxylase

Monooxygenase

Rhodococcus jostii RHA1

ABSTRACT

The genome of *Rhodococcus jostii* RHA1 contains an unusually large number of oxygenase encoding genes. Many of these genes have yet an unknown function, implying that a notable part of the biochemical and catabolic biodiversity of this Gram-positive soil actinomycete is still elusive. Here we present a multiple sequence alignment and phylogenetic analysis of putative *R. jostii* RHA1 flavoprotein hydroxylases. Out of 18 candidate sequences, three hydroxylases are absent in other available *Rhodococcus* genomes. In addition, we report the biochemical characterization of 3-hydroxybenzoate 6-hydroxylase (3HB6H), a gentisate-producing enzyme originally mis-annotated as salicylate hydroxylase. *R. jostii* RHA1 3HB6H expressed in *Escherichia coli* is a homodimer with each 47 kDa subunit containing a non-covalently bound FAD cofactor. The enzyme has a pH optimum around pH 8.3 and prefers NADH as external electron donor. 3HB6H is active with a series of 3-hydroxybenzoate analogues, bearing substituents in *ortho*- or *meta*-position of the aromatic ring. Gentisate, the physiological product, is a non-substrate effector of 3HB6H. This compound is not hydroxylated but strongly stimulates the NADH oxidase activity of the enzyme.

© 2011 Elsevier B.V. All rights reserved.

1. Introduction

Rhodococcus jostii RHA1 is a Gram-positive soil actinomycete able to degrade a wide range of organic compounds [1–4]. It possesses one of the largest bacterial genomes ever sequenced and encodes an exceptional amount of oxygenases (203 putative genes), in particular flavoprotein monooxygenases (88 putative genes) [5].

Flavoprotein monooxygenases (EC 1.14.13.x) perform a wide range of regio- and enantioselective reactions and can be divided in six subclasses [6]. Subclass A comprises a family of single-component flavoprotein hydroxylases, which are crucially involved in microbial degradation of natural and anthropogenic aromatics [7–9], polyketide antibiotic biosynthesis [10–12], and antibiotic resistance [13–15].

Flavoprotein hydroxylases can be identified on the basis of three fingerprint sequences, first defined in 4-hydroxybenzoate 3-hydroxylase (PHBH) (Fig. 1) [16]. The GxGxxG sequence motif maps the ADP moiety of FAD [17], while the GD consensus motif represents the residues that interact with the riboflavin moiety of FAD [18]. Both of these FAD fingerprints are common for many flavoproteins [19]. The third, DG consensus motif, is specific for subclass A enzymes and serves a dual role of recognition of both FAD and NADPH [16].

Here we used the above mentioned fingerprints to detect putative flavoprotein hydroxylase sequences in the *R. jostii* RHA1 genome (Fig. 1; Table 1). Since most of the retrieved sequences are annotated

without a particular function, we performed a multiple sequence alignment and phylogenetic analysis with a large set of known flavoprotein hydroxylases. Among the newly assigned functions, we present the biochemical characterization of 3-hydroxybenzoate 6-hydroxylase (3HB6H), a flavoprotein involved in the gentisate (2,5-dihydroxybenzoate) degradation pathway [20, 21]. Notably, the gene encoding for this flavoenzyme is mis-annotated as a salicylate (2-hydroxybenzoate) hydroxylase. *R. jostii* RHA1 3HB6H expressed in *Escherichia coli* is specific for 3-hydroxybenzoate derivatives and does not interact with salicylate.

2. Materials and methods

2.1. Chemicals

DNAseI was from Boehringer Mannheim GmbH (Mannheim, Germany). Restriction endonucleases and dNTPs were purchased from Invitrogen (Carlsbad, CA, USA). Phusion High Fidelity DNA polymerase was from Finnzymes (Espoo, Finland). In-Fusion PCR cloning System was purchased from Clontech (Mountain View, CA, USA). Oligonucleotides were synthesised by Eurogentec (Liege, Belgium). *E. coli* TOP10 was from Invitrogen (Carlsbad, CA, USA). The pBAD/Myc-His (Nde) expression vector was kindly provided by Prof. M.W. Fraaije (University of Groningen).

Nickel nitrilotriacetic acid (Ni-NTA) agarose was purchased from Qiagen (Valencia, CA, USA) and Bio-Gel P-6DG was from Bio-Rad (Hercules, CA, USA). HiLoad 26/10 Q-Sepharose HP, Superdex 200 HR10/30, low molecular weight protein marker, prestained kaleidoscope

* Corresponding author. Tel.: +31 317 482861; fax: +31 317 484801.

E-mail address: willem.vanberkel@wur.nl (W.J.H. van Berkel).

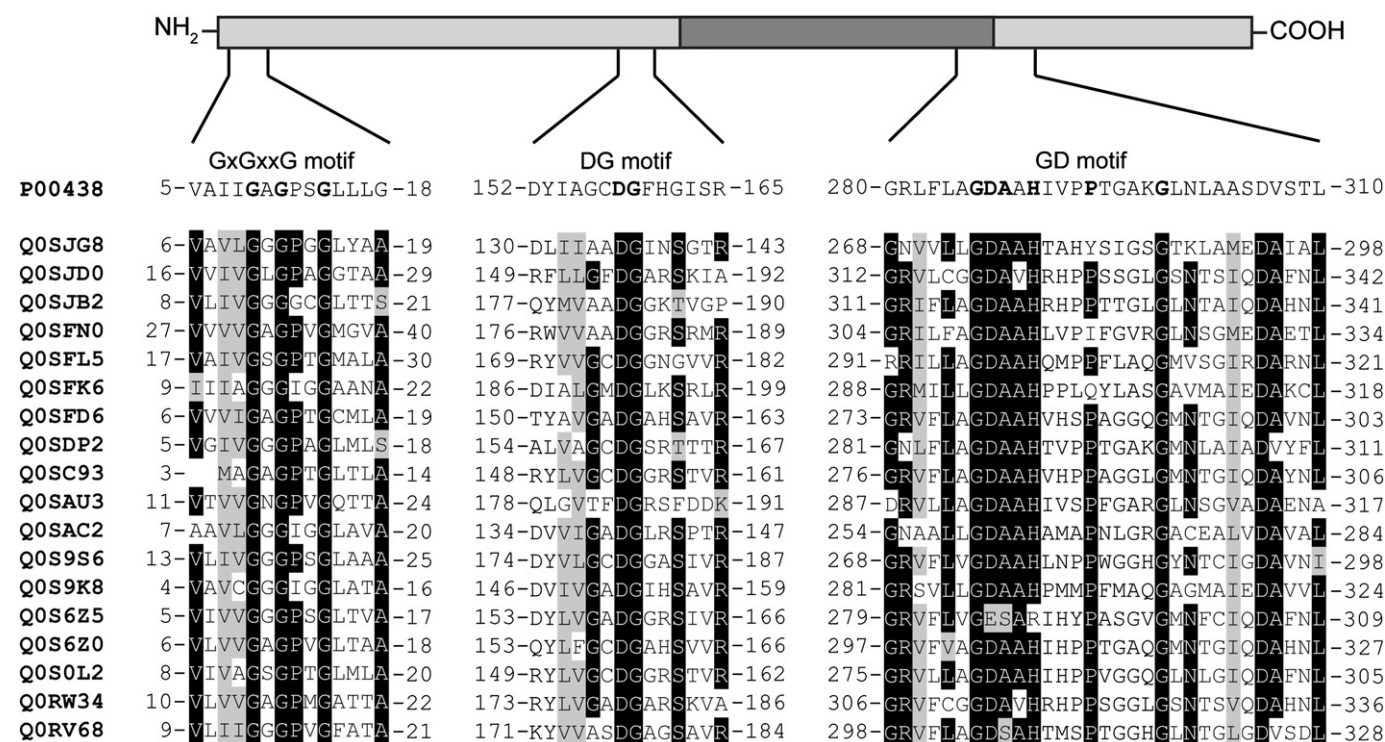


Fig. 1. Sequence comparison of putative flavoprotein hydroxylases from *Rhodococcus jostii* RHA1. Upper panel: Schematic representation of the primary structure of PHBH from *P. fluorescens* (UniProt ID: P00438) with the FAD-binding domain in light gray and the substrate binding domain in dark gray. Middle panel: Schematic representation of the flavoprotein hydroxylase fingerprints of PHBH from *P. fluorescens* used in this study. Bold characters represent residues used for fingerprinting. Lower panel: Sequence alignment of flavoprotein hydroxylase fingerprint regions among putative flavoprotein hydroxylases from *R. jostii* RHA1. Identical residues are shaded in black, similar residues are shaded in gray.

protein standards, and catalase (232 kDa), aldolase (158 kDa), BSA (68 kDa) and ovalbumin (43 kDa) were obtained from Pharmacia Biotech (Uppsala, Sweden).

Aromatic compounds were purchased from Sigma-Aldrich (St Louis, MO, USA) and Acros Organics (New Jersey, US). Catalase, FAD, FMN, riboflavin and arabinose were from Sigma-Aldrich (St Louis, MO, USA). Pefabloc SC was obtained from Roche Diagnostics GmbH (Mannheim, Germany). All other chemicals were from commercial sources and of the purest grade available.

2.2. Sequence analysis

The genome of *R. jostii* RHA1 was analysed for the presence of flavoprotein hydroxylases at the European Bioinformatic Institute (www.ebi.ac.uk). FASTA analysis (www.ebi.ac.uk/Tools/sss/fasta) was performed to determine protein sequence homology. Multiple sequence alignments were made using CLUSTALW [22]. DNA cluster comparison and database searches were carried out using Nucleotide and Protein resources from the National Center for Biotechnology Information (www.ncbi.nlm.nih.gov) and UniProt Database (www.uniprot.org). Phylogenetic analysis was performed using FigTree (tree.bio.ed.ac.uk).

2.3. Cloning, expression and purification of 3-hydroxybenzoate 6-hydroxylase in *E. coli*

A 1.2 kb DNA fragment encoding a putative salicylate hydroxylase (Gene ID: 4218663) was PCR amplified from *R. jostii* RHA1 genomic DNA, using the oligonucleotides SM_1869fwd (5'AGGAGGAAT-TACATATGTCGAATCTGCAGGACGCAC3') and SM_1869rev (5'GTTCG-GGCCAAAGCTTTGACGCGGATCGGACG3'), introducing *Nde*I and *Hind*III restriction sites (underlined), respectively and containing the start codon (bold). The amplified fragment was cloned into the pBAD/Myc-His expression vector containing a C-terminal His₆-tag by using the In-Fusion PCR Cloning System. The resulting construct

(pBAD-3HB6H-His₆) was verified by automated sequencing of both strands and electroporated to *E. coli* TOP10 cells for recombinant expression.

The Äkta Explorer FPLC system (Pharmacia Biotech) was used for protein chromatography. For enzyme production, *E. coli* TOP10 cells, harbouring a pBAD-3HB6H plasmid, were grown in TB medium supplemented with 100 µg mL⁻¹ ampicillin until an optical density (OD_{600 nm}) of 0.8 was reached. Expression was induced by the addition of 0.02% (w/v) arabinose and the incubation was continued for 16 h at 37 °C. Cells (36 g wet weight) were harvested by centrifugation, resuspended in 120 mL of 20 mM potassium phosphate, 300 mM NaCl (pH 7.4), containing 1 mM Pefabloc SC, 1 mg DNase, 100 µM MgCl₂ and subsequently passed twice through a precooled French Pressure cell (SLM Aminco, SLM Instruments, Urbana, IL, USA) at 16,000 psi. The resulting homogenate was centrifuged at 25,000 g for 45 min at 4 °C to remove cell debris, and the supernatant was applied onto a Ni-NTA agarose column (13 × 1.6 cm) equilibrated with 20 mM sodium phosphate, 300 mM NaCl (pH 7.4). The column was washed with two volumes of equilibration buffer. The enzyme was eluted with 300 mM imidazole in equilibration buffer. The active pool, containing an added excess of free FAD, was desalted using a Biogel column (14 × 2.6 cm), running in 50 mM BisTris-HCl, 0.1 mM EDTA (pH 7.2). The desalted protein was loaded onto a HiLoad 26/10 Q-Sepharose HP column equilibrated with the same buffer. After washing with two column volumes of starting buffer, the protein was eluted with a linear gradient of NaCl (0–1 M) in the same buffer. Active fractions were pooled and concentrated to 8 mg/mL by using Amicon filters (30 kDa cutoff) and dialysed at 4 °C against 50 mM BisTris-HCl (pH 7.2). Purified 3HB6H was frozen in liquid nitrogen and stored at –80 °C.

2.4. Protein analysis

SDS/PAGE was performed using 12.5% acrylamide slab gels essentially as described by Laemmli [23]. Proteins were stained using

Table 1Flavoprotein hydroxylases from *R. jostii* RHA1.

Locus name	TrEMBL	Annotated name	Putative function from NJ-tree ^a (EC number)	Presence in other <i>Rhodococcus</i> sp (percentage identity).
RHA1_ro00482	Q0SJG8	Monoxygenase/aromatic ring hydroxylase	Acting on activated substrate	<i>R. opacus</i> B4 (74)
RHA1_ro00520	Q0SJD0	3-(2-hydroxyphenyl) propionate monoxygenase	3-(2-hydroxyphenyl) propionate hydroxylase (EC 1.14.13.x)	<i>R. aetherivorans</i> (90)
RHA1_ro00538	Q0SJB2	Aromatic ring hydroxylase		<i>R. opacus</i> B4 (96)
RHA1_ro01845	Q0SFN0	Probable aromatic ring hydroxylase		<i>R. erythropolis</i> TA421 (78)
				<i>R. opacus</i> B4 (93)
				<i>R. equi</i> ATCC 33707 (72)
				<i>R. equi</i> 103S (72)
				<i>R. erythropolis</i> SK121 (71)
				<i>R. erythropolis</i> PR4 (70)
RHA1_ro01860	Q0SFL5	Probable 3-(3-hydroxyphenyl) propionate hydroxylase		<i>R. opacus</i> B4 (40)
RHA1_ro01869	Q0SFK6	Probable salicylate monoxygenase	3-hydroxybenzoate 6-hydroxylase (EC 1.14.13.24)	<i>R. opacus</i> B4 (96)
RHA1_ro01939	Q0SFD6	Pentachlorophenol monoxygenase		<i>Rhodococcus</i> NCIMB 12038 (93)
RHA1_ro02539	Q0SPD2	4-hydroxybenzoate 3-monoxygenase	4-hydroxybenzoate 3-hydroxylase (EC 1.14.13.2)	<i>R. opacus</i> B4 (90)
				<i>R. opacus</i> B4 (97)
				<i>R. equi</i> ATCC 33707 (88)
				<i>R. equi</i> 103S (87)
				<i>R. erythropolis</i> SK121 (89)
				<i>R. erythropolis</i> PR4 (87)
RHA1_ro03040	Q0SC93	Probable aromatic ring hydroxylase		<i>R. opacus</i> B4 (92)
RHA1_ro03540	Q0SAU3	Pentachlorophenol monoxygenase		<i>R. opacus</i> B4 (90)
RHA1_ro03714	Q0SAC2	Possible aromatic ring hydroxylase		<i>R. opacus</i> B4 (95)
				<i>R. equi</i> ATCC 33707 (60)
				<i>R. equi</i> 103S (60)
RHA1_ro03910	Q0S9S6	FAD-binding monoxygenase		
RHA1_ro03981	Q0S9K8	Probable aromatic ring monoxygenase	6-hydroxynicotinate 3-monoxygenase (EC 1.14.13.114)	<i>R. opacus</i> B4 (93)
RHA1_ro04910	Q0S6Z5	Monoxygenase		
RHA1_ro04915	Q0S6Z0	Monoxygenase		<i>R. opacus</i> B4 (94)
				<i>R. erythropolis</i> SK121 (63)
				<i>R. erythropolis</i> PR4 (63)
RHA1_ro07160	Q0S0L2	Probable FAD-dependent monoxygenase	Rifampicin monoxygenase (1.14.13.x)	<i>R. opacus</i> B4 (73)
				<i>R. equi</i> ATCC 33707 (73)
				<i>R. equi</i> 103S (73)
				<i>R. erythropolis</i> SK121 (69)
				<i>R. erythropolis</i> PR4 (69)
				<i>Rhodococcus</i> NCIMB 9874 (80)
RHA1_ro10313	Q0RW34	Probable 2,4-dichlorophenol 6-monoxygenase	3-(2-hydroxyphenyl) propionate hydroxylase (EC 1.14.13.x)	<i>R. aetherivorans</i> (59)
RHA1_ro11171	Q0RV68	Possible monoxygenase/hydrolase		

^a Neighbour joining tree (Fig. 2).

Coomassie Brilliant Blue R-250. Total protein concentrations were estimated using the BCA protein kit from Thermo Scientific Pierce with BSA as standard. Analytical gel filtration to investigate the hydrodynamic properties of 3HB6H was performed on a Superdex 200 HR 10/30 column running in 50 mM potassium phosphate, 150 mM KCl (pH 7.4). Desalting or buffer exchange of small aliquots of enzyme was performed with Bio-Gel P-6DG columns and Amicon Ultra-0.5 filters (30 kDa cut off) (Millipore).

2.5. Spectral analysis

Absorption spectra were recorded at 25 °C on a Hewlett Packard (Loveland, CO, USA) 8453 diode array spectrophotometer in 50 mM Tris-SO₄ (pH 8.0). Spectra were analysed using the UV-Visible CHEMSTATION software package (Hewlett Packard).

The molar absorption coefficient of protein-bound FAD was determined by recording the absorption spectrum of 3HB6H in the presence and absence of 0.1% (w/v) SDS, assuming a molar absorption coefficient for free FAD of 11.3 mM⁻¹ cm⁻¹ at 450 nm. Purified enzyme concentrations were routinely determined by measuring the absorbance at 453 nm using the molar absorption coefficient for protein-bound FAD (10.3 mM⁻¹ cm⁻¹).

2.6. HPLC product analysis

The enzymatic conversions were analysed by HPLC using an Applied Biosystems 400 pump equipped with a Waters 996 photodiode-

array detector. Reaction products were separated with a 4.0 × 60 mm C18 reverse-phase column (Spherisorb, ODS 2, Pharmacia). Reaction mixtures contained 2 mM substrate, 5 mM of NADH and 2 μM 3HB6H in 1.5 mL air saturated 20 mM Tris-SO₄ pH 8.0. At the end of the reaction, 10 kDa spin filters were used to separate the enzyme from the reaction mixture. HPLC analysis of the resulting supernatant was carried out by gradient elution with 0.8% acetic acid and 20% methanol (pH 2.9) as mobile phase (flow rate 0.8 mL/min).

2.7. Cofactor determination

The flavin cofactor of 3HB6H was identified by thin layer chromatography (TLC). The cofactor was released from the protein by boiling for 5 min or acid treatment. The protein precipitate was removed by centrifugation and the supernatant was applied together with the reference compounds FAD, FMN and riboflavin onto a TLC plate (Baker-flex Silica Gel 1B2; JT Baker Inc., Phillipsburg, NY, USA). Butanol/acetic acid/water (5:3:3) served as the mobile phase.

2.8. Enzyme activity

3HB6H activity was routinely assayed by following the decrease in absorbance of NADH at 360 nm at 25 °C on a Hewlett Packard 8453 diode array spectrophotometer. Initial velocity values were calculated using a molar absorption coefficient (ε₃₆₀) of 4.31 mM⁻¹ cm⁻¹. The standard assay mixture contained 50 mM Tris-SO₄ (pH 8.0), 200 μM 3-hydroxybenzoate and 250 μM NADH; the reaction was started by

addition of 45 nM enzyme. One unit of enzyme activity (U) is defined as the amount of enzyme that consumes 1 μmol of NADH per min. The optimal pH for activity of 3HB6H was determined using 25 mM MES, HEPES and CHES buffers with varying pH (pH 5.5–9.5) and adjusted to an ionic strength of 0.1 M with Na_2SO_4 [24].

The activity of 3HB6H with 3-hydroxybenzoate, 2,3-dihydroxybenzoate, 3,5-dihydroxybenzoate and 2,5-dihydroxybenzoate followed Michaelis–Menten kinetics [25]. Kinetic parameters were calculated from multiple measurements with various substrate concentrations using a direct nonlinear regression fit to the data.

2.9. Oxygen consumption

An OxyTherm Clark-type oxygen electrode system (Hansatech, Norfolk, UK) was used to determine the hydroxylation efficiency of 3HB6H towards different substrates. The assay solution (final volume 1.0 mL) contained 350 μM substrate, 250 μM NADH and 1 μM 3HB6H in 50 mM air saturated Tris– SO_4 (pH 8.0) at 25 °C. At the end of the reaction, the amount of hydrogen peroxide produced was determined by adding 0.02 mg/mL of catalase ($2 \text{H}_2\text{O}_2 \rightarrow \text{O}_2 + 2 \text{H}_2\text{O}$).

2.10. Substrate binding studies

The interaction of 3HB6H (25 μM) with substrate analogues was studied in 50 mM Tris– SO_4 (pH 8.0). Dissociation constants (K_d) of enzyme/substrate complexes were determined from flavin absorption difference spectra. The K_d was calculated from the changes in absorbance at 490 nm using a direct nonlinear regression fit to the data with IGOR (Wavemetrics, Lake Oswego, OR, USA). Apparent dissociation constants were calculated by fitting the relative absorbencies to Eq. (1), a modified equation compared with the one described elsewhere [26]:

$$A_{490} = \varepsilon_{ES} * ES + \varepsilon_E * (E_t - ES) \quad (1)$$

where

$$ES = \left[(E_t + S_t + K_d) - \sqrt{(E_t + S_t + K_d)^2 - 4ES} \right] / 2$$

and A_{490} , E_t , S_t , ES , K_d , ε_{ES} , ε_E are the absorbances observed at 490 nm, the total enzyme concentration, the total substrate concentration, the enzyme–substrate complex concentration, the dissociation constant of the enzyme–substrate complex, the molar absorption coefficient of the enzyme–substrate complex and the molar absorption coefficient of the free enzyme, respectively.

3. Results

3.1. Analysis of *R. jostii* RHA1 genome

3.1.1. Identification of *R. jostii* RHA1 flavoprotein hydroxylases

By searching the *R. jostii* RHA1 genome with the three flavoprotein hydroxylase fingerprints of PHBH from *Pseudomonas fluorescens* (Fig. 1) [16], we retrieved eighteen candidate sequences (Fig. 1 and Table 1). Out of the candidate sequences, fifteen are present in other sequenced *Rhodococcus* strains with highest similarities found in *Rhodococcus opacus* B4. Q0S9S6, Q0S6Z5 and Q0RV68 are only present in *R. jostii* RHA1. From the alignments it is clear that the consensus sequences of the selected proteins are well conserved, even though small deviations occur.

3.1.2. Multiple sequence alignment and phylogenetic tree analysis

Most of the retrieved sequences are not linked to a clear annotated function. To predict protein functions, we performed a multiple sequence alignment and phylogenetic analysis with characterised flavoprotein

hydroxylases from different bacterial orders and some eukaryotic systems (see Supporting Table S1 for complete UniProt ID list). The neighbour joining method was used to draw the phylogenetic tree (Fig. 2).

Among the retrieved sequences, only two annotated functions (Q0SJD0 and Q0SPD2) were confirmed by phylogenetic analysis. Q0SJD0 encodes for 3-(2-hydroxyphenyl) propionate hydroxylase, an enzyme characterised solely in *Rhodococcus aetherivorans* [27]. Q0SPD2 encodes for 4-hydroxybenzoate 3-hydroxylase, the prototype of the flavoprotein hydroxylase family [28]. Q0SAU3 and Q0SFD6 are annotated as pentachlorophenol monooxygenases but neither cluster with the characterised pentachlorophenol-converting enzymes.

Eleven sequences are annotated either as putative monooxygenase, FAD binding monooxygenase or aromatic ring hydroxylase. From our analysis, putative functions can be assigned to Q0SJG8, Q0S9K8 and Q0S0L2. Q0SJG8 clusters with a group of flavoproteins acting on activated substrates, including among others salicylyl-CoA 5-hydroxylase (Q7X281) and 2-aminobenzoyl-CoA monooxygenase/reductase (Q93FB38, Q93FC6), acting on CoA-activated salicylate and CoA-activated 2-aminobenzoate, respectively. Another member of this group is the newly identified enzyme SibG that acts on an activated form of sibiromycin [29]. Q0S9K8 might encode for 6-hydroxynicotinate 3-monooxygenase (39% sequence identity and 56% similarity), since it belongs to the 6-hydroxynicotinate 3-monooxygenase clade, where two enzymes both from *Pseudomonas* have been characterised [30, 31]. Q0S0L2 has high sequence homology with rifampicin monooxygenase, an enzyme present in actinomycetes such as *Rhodococcus equi* and *Nocardia farcinica* [13, 14].

Three sequences have been annotated with a probable enzymatic function but all of them seem mis-annotated. According to the phylogenetic tree, Q0RW34 encodes for a 3-(2-hydroxyphenyl) propionate hydroxylase instead of 2,4-dichlorophenol 6-monooxygenase. Three different types of 2,4-dichlorophenol 6-monooxygenases are known [32–34], but Q0RW34 does not cluster with any of them. Q0SFL5 does not seem to encode for a 3-(3-hydroxyphenyl) propionate hydroxylase, since the sequence outgroups from the clade quite early. Therefore, no putative function for Q0SFL5 can be addressed. Finally, Q0SFK6 is annotated as a putative salicylate hydroxylase, but both sequence alignment and cluster analysis (Fig. 2) support another function (see Section 3.2).

3.2. Functional annotation of 3HB6H

3.2.1. Gene order conservation

Putative salicylate monooxygenase (RHA1_ro01869, GENE ID: 4218663) DNA locus region contains genes belonging to the gentisate degradation pathway (Fig. 3): RHA1_ro01866 (GENE ID: 4218660) encodes for a ring-fission dioxygenase that converts gentisate to maleylpyruvate. This product is further converted to fumarylpyruvate by a maleylpyruvate isomerase encoded by RHA1_ro01865 (GENE ID: 4218659). DNA regions encoding for known 3HB6Hs possess the same gene order organisation as the RHA1_ro01869 DNA region, especially the 3HB6H degradation operon from *Corynebacterium glutamicum* (Fig. 3) [33, 34]. Q0SFK6 shares 93% amino acid sequence identity with 3HB6H from *Rhodococcus* NCIMB 12038 (*narX*, GenBank: HM852512.1) [35] and 96% with putative 3HB6H from *R. opacus* B4 (ROP_15470, GENE ID: 7741586). Thus, based on protein sequence similarity, phylogenetic tree clustering and gene order conservation, we hypothesised that Q0SFK6 encodes for 3HB6H instead of salicylate hydroxylase. Very recently, a homologue 3HB6H gene was identified in *Candida parapsilosis* [36]. The *C. parapsilosis* 3HB6H sequence does not cluster with bacterial 3HB6Hs (Fig. 2). Instead, it forms a separate clade together with 4-hydroxybenzoate 1-hydroxylase from the same fungus [36, 37], probably due to the common eukaryotic origin.

3.2.2. Cloning, expression and purification of Q0SFK6

To assess the activity of Q0SFK6, the gene was cloned into vector pBAD/Myc-His under control of the inducible *ara* promoter. The

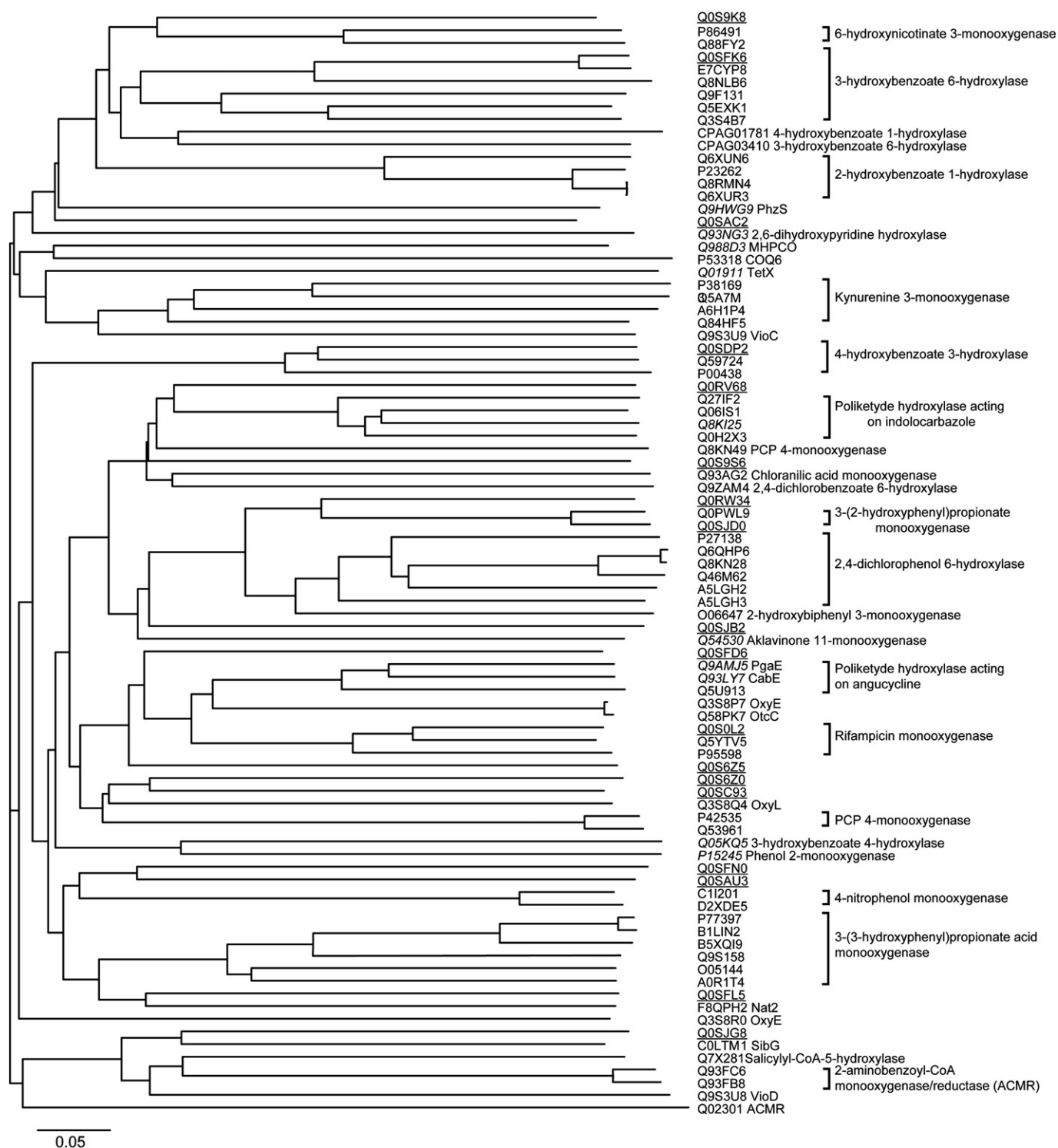


Fig. 2. Neighbour-joining tree of flavoprotein hydroxylases. Underlined UniProt IDs represent hydroxylases from *R. jostii* RHA1. Italics UniProt IDs are sequences of hydroxylases with known crystal structures. On the right, enzymatic function has been reported. For the complete list of sequences used see supporting information (Supporting Table S1).

expression vector was transformed in *E. coli* TOP10 cells and overexpression of the His-tagged protein was induced by adding 0.02% (w/v) arabinose to the Terrific Broth medium. High level of expression was found after 16 h of induction at 37 °C. No expression was achieved in Luria Bertani medium. The recombinant protein was purified to apparent homogeneity by two successive chromatographic steps (Table 2). Approximately 420 mg of recombinant Q0SFK6 protein could be purified from 6 L batch culture containing 36 g (wet weight) of cells. SDS-PAGE showed a single band with an apparent

molecular mass of 47 kDa (Fig. 4A), in agreement with the Q0SFK6 amino acid sequence. The relative molecular mass of the native recombinant protein was estimated to be ~108 kDa by analytical gel filtration (Fig. 4B), which indicates a dimer conformation in solution.

3.2.3. Spectral properties

Recombinant Q0SFK6 showed a typical flavoprotein absorption spectrum with maxima at 274 nm, 383 nm and 453 nm and a shoulder at 480 nm (Fig. 5A). The molar absorption coefficient of protein-

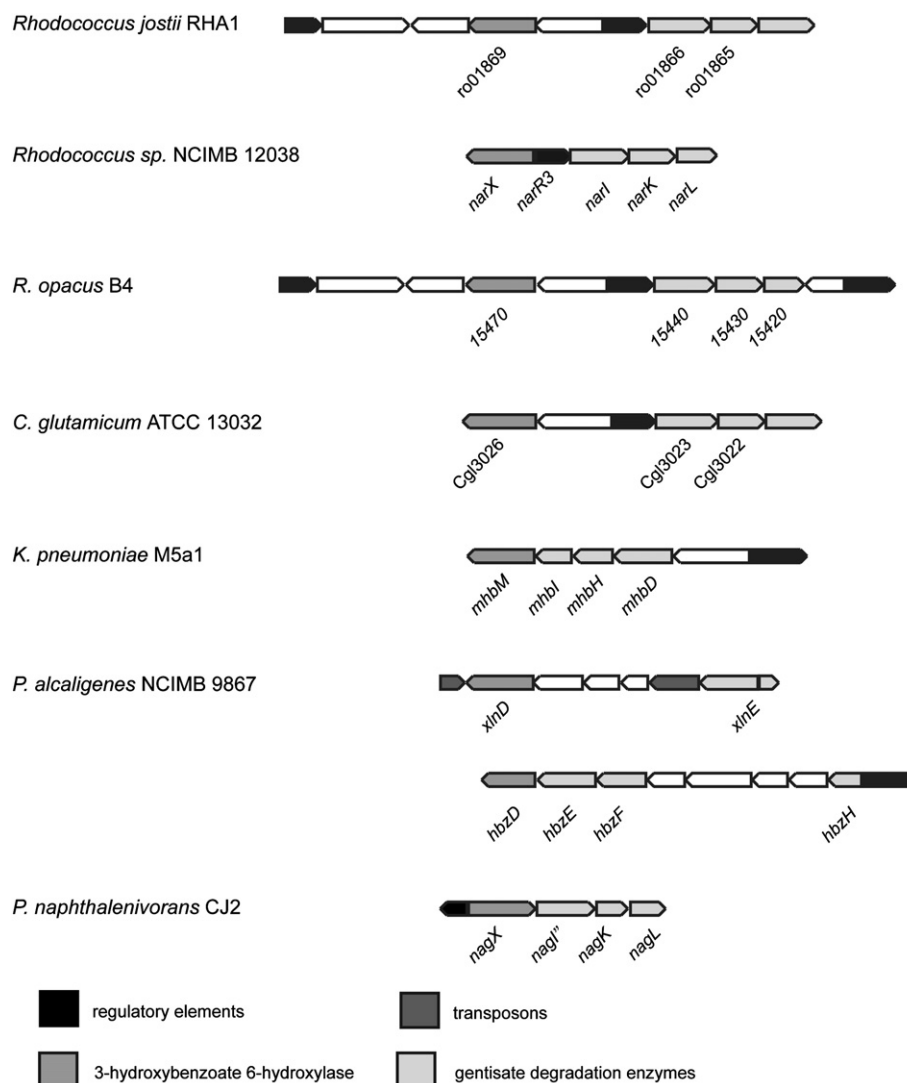


Fig. 3. Physical maps of gene clusters encoding for 3-hydroxybenzoate and gentisate degradation. ORFs annotated as unknown function are depicted in white. The sequences were taken from (GenBank ID) *R. jostii* RHA1 (CP000431), *Rhodococcus. sp.* NCIMB 12083 (HM852512), *R. opacus* B4 (NC_012522), *C. glutamicum* ATCC13032 (BA000036), *K. pneumoniae* M5a1 (AY648560), *P. alcaligenes* NCIMB 9867 (AF173167, DQ394580) and *P. naphthalenivorans* CJ2 (DQ167474).

bound flavin was determined to be $10.3 \text{ mM}^{-1} \text{ cm}^{-1}$ at 453 nm. The A_{274}/A_{453} ratio of the FAD-saturated protein preparation was 11.9. The A_{383}/A_{453} ratio (Fig. 5A) is 1.2, a rather high value for flavoproteins. The flavin cofactor could be released from the protein by boiling or acid treatment and was identified as FAD by TLC.

3.3. Catalytic properties of 3HB6H

3.3.1. Enzyme activity and product analysis

Enzyme activity was assayed by measuring the consumption of NADH spectrophotometrically. QOSFK6 showed a very low NADH oxidase activity ($<1 \text{ U mg}^{-1}$). No increase in enzyme activity was detected in the presence of salicylate, while NADH consumption

was strongly stimulated by 3-hydroxybenzoate. The aromatic product was identified as gentisate (2,5-dihydroxybenzoate) by absorption spectral analysis, and HPLC (Table 4). Thus, enzyme activity and product analysis confirms the new annotation of QOSKF6 as 3-hydroxybenzoate 6-hydroxylase (3HB6H).

3.3.2. Kinetic parameters

3HB6H from *R. jostii* RHA1 catalyses the *para*-hydroxylation of 3-hydroxybenzoate with the consumption of NAD(P)H and oxygen. The enzyme displayed a maximum activity around pH 8.0 in Tris- SO_4 buffer and around pH 8.6 in HEPES buffer (data not shown). Like other flavoprotein hydroxylases [38–40], the enzyme was strongly inhibited by chloride ions. The steady-state kinetic parameters of 3HB6H were determined at 25 °C in 50 mM Tris- SO_4 (pH 8.0) (Table 3). This analysis revealed that the enzyme clearly prefers NADH ($K_m = 48 \pm 4 \mu\text{M}$) over NADPH ($K_m = 390 \pm 80 \mu\text{M}$) as external electron donor.

3.3.3. Substrate and effector specificity

3HB6H from *R. jostii* RHA1 catalyses the regioselective *para*-hydroxylation of 3-hydroxybenzoate forming gentisate (Fig. 6). Besides the parent substrate, 3HB6H was most active with 2,3-dihydroxybenzoate and 3,5-dihydroxybenzoate (Table 3; Fig. 6).

Table 2
Purification of *R. jostii* RHA1 QOSFK6 expressed in *E. coli*.

Step	Protein (mg)	Activity (U)	Specific activity (U mg^{-1})	Yield %
Cell extract	3360	18,718	6	100
Ni-NTA agarose	780	14,997	19	80
Q-Sepharose	450	10,738	24	57

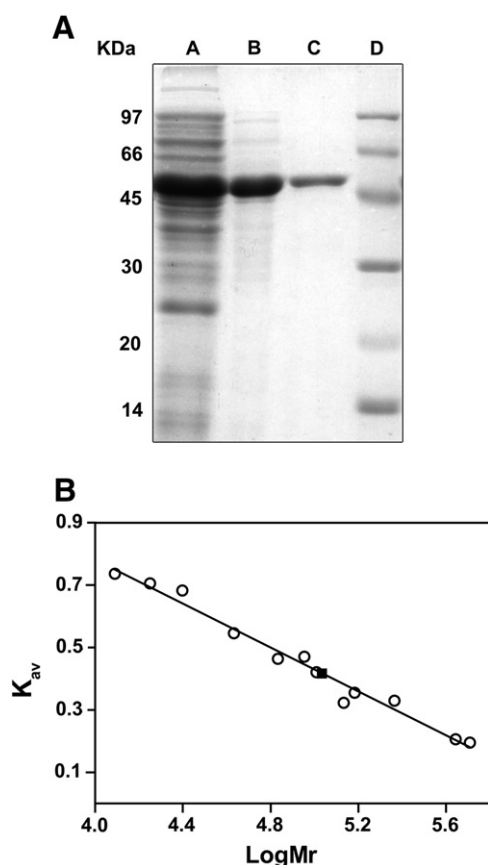


Fig. 4. Hydrodynamic properties of 3HB6H. A) SDS/PAGE analysis of the purification of 3HB6H from *R. jostii* RHA1 expressed in *E. coli*. Lane A, cell extract; Lane B, Ni-NTA pool; Lane C, Q-sepharose pool; Lane D, low molecular weight marker. B) Analytical gel filtration. Reference proteins used to calibrate the column and calculate the 3HB6H apparent molecular mass: cytochrome c (12.3 kDa), myoglobin (17.8 kDa), α -chymotrypsin (25 kDa), ovalbumin (43 kDa), bovine serum albumin (68 and 136 kDa), 4-hydroxybenzoate 3-hydroxylase (90 kDa), lipoamide dehydrogenase (102 kDa), phenol 2-hydroxylase (152 kDa), catalase (232 kDa), ferritin (440 kDa) and vanillyl-alcohol oxidase (510 kDa); ■ 3HB6H.

Next to that, the enzyme slowly converted ($k_{\text{cat}} < 5 \text{ s}^{-1}$) a number of 3-hydroxybenzoate derivatives with substituents at the 4-position (Table 4). Among these compounds, 3,4-dihydroxybenzoate is a very poor substrate (Table 4). In analogy with the conversion of 2,3,4-trihydroxybenzoate to 2,3,4,6-tetrahydroxybenzoate, the enzyme transformed the initial product of the reaction with 3,5-dihydroxybenzoate (2,3,5-trihydroxybenzoate) to 2,3,5,6-tetrahydroxybenzoate (Table 4).

To discriminate between true substrates and non-substrate effectors, oxygen consumption experiments were performed in the absence and presence of catalase. With all substrates, a certain degree of uncoupling of hydroxylation was observed, as evidenced by the production of hydrogen peroxide (Table 3). Gentsitate, the physiological product, is a good effector of 3HB6H. This compound is not converted but strongly stimulates the NADH oxidase activity of the enzyme (Fig. 6).

3.3.4. Substrate binding

Upon titration of 3HB6H with 3-hydroxybenzoate derivatives, characteristic perturbations in the absorption properties of the FAD cofactor were observed (Fig. 5B). From the absorption differences around 490 nm, dissociation constants (K_d values) were estimated for the binary enzyme–substrate complexes (Table 3). Similar titration experiments with salicylate established that this compound does not induce any flavin absorption change (data not shown).

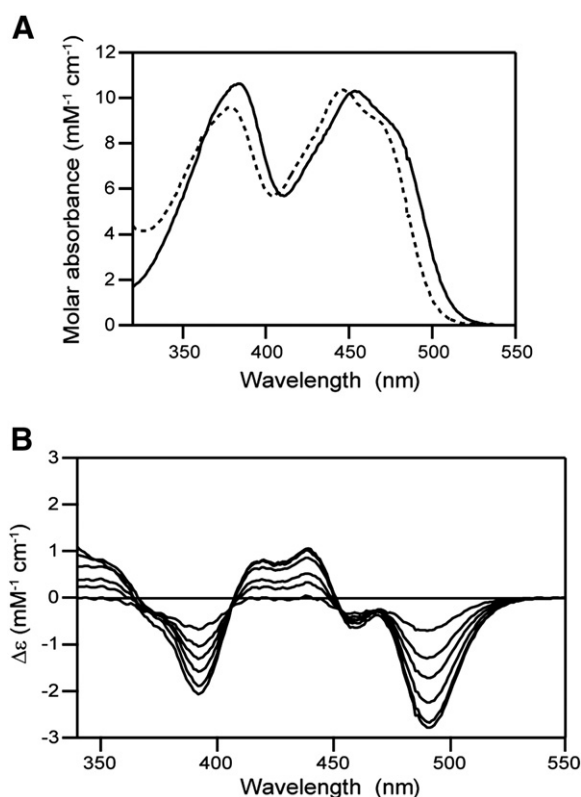


Fig. 5. Spectral properties of 3HB6H. A) Absorption spectra of free 3HB6H (solid line) and 3HB6H in complex with 890 μM 3-hydroxybenzoate (dashed line). The enzyme concentration was 25 μM . B) Absorption difference spectra observed upon binding of 3-hydroxybenzoate to 25 μM 3HB6H. The curves shown are the difference spectra, the corrected enzyme spectra in the presence of 17, 50, 82, 177, 455 and 890 μM 3-hydroxybenzoate, minus the enzyme spectrum in the absence of 3-hydroxybenzoate. All experiments were performed in 50 mM Tris– SO_4 (pH 8.0).

4. Discussion

R. jostii RHA1 is a versatile Gram-positive soil bacterium degrading a wide range of organic compounds, including lignin [1]. It contains an impressive amount of oxygenases, especially flavoprotein monooxygenases. Recently, Szolkowy and colleagues characterised the Baeyer–Villiger monooxygenase (BMVO) subclass of *R. jostii* RHA1 pointing out an exceptional diversity in regio- and enantioselectivity [41].

In the present study, we searched for new flavoprotein hydroxylases in the *R. jostii* RHA1 genome. Most of these enzymes are single-component proteins that form a specific class of flavoprotein monooxygenases (subclass A). By using three different fingerprints we were able to retrieve eighteen candidate flavoprotein hydroxylase sequences. Three of these sequences turned out to be *R. jostii* RHA1 specific, while the others are present also in other available

Table 3
Substrate and effector specificity of 3HB6H.

Substrate	K_d (μM)	K_m (μM)	k_{cat} (s^{-1})	k_{cat}/K_m ($\text{M}^{-1} \text{s}^{-1}$)	Uncoupling (%)
3-hydroxybenzoate	48 ± 2	46 ± 3	35 ± 1	8×10^5	5
3,5-dihydroxybenzoate	310 ± 60	250 ± 10	13 ± 1	5×10^4	10
2,3-dihydroxybenzoate	63 ± 9	51 ± 7	10 ± 1	2×10^5	20
2,5-dihydroxybenzoate	190 ± 10	140 ± 30	7 ± 1	5×10^4	99

Apparent kinetic constants were determined at 25 °C in 50 mM Tris– SO_4 (pH 8.0). Values are presented as the mean of three experiments. The percentage of uncoupling of hydroxylation was determined from polarographic measurements using a Clarke-type electrode. The percentage of uncoupling equals twice the amount of oxygen, produced after addition of catalase at the end of the reaction ($2 \text{H}_2\text{O}_2 \rightarrow \text{O}_2 + 2 \text{H}_2\text{O}$).

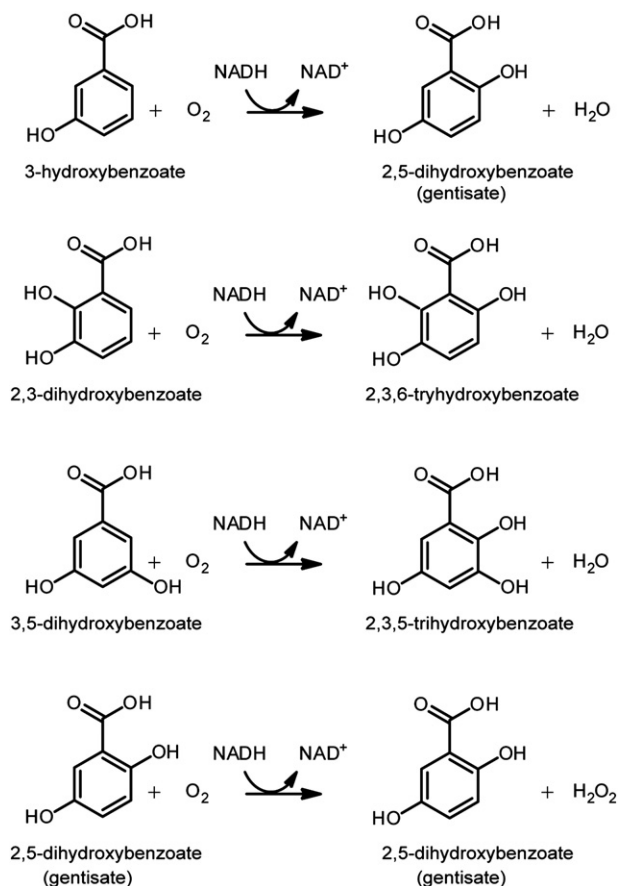


Fig. 6. Reactions catalyzed by 3HB6H. From top to bottom: reactions with the best substrates (3-hydroxybenzoate, 2,3-dihydroxybenzoate and 3,5-dihydroxybenzoate) and the best non-substrate effector (2,5-dihydroxybenzoate).

Rhodococcus genomes, especially in *R. opacus* strain B4. The highest sequence similarity with flavoprotein hydroxylases from *R. opacus* strain B4 is in agreement with the overall synteny between these *Rhodococcus* strains.

Most of the candidate flavoprotein hydroxylase sequences have been annotated without a specific function or are mis-annotated. From multiple sequence alignment and phylogenetic analysis we could assess some new putative functions.

Q0S0L2 encodes for a rifampicin monooxygenase, an enzyme able to decompose the antibiotic via *N*-hydroxylation. This type of decomposition mechanism is driven by flavoprotein monooxygenases in *N. farcinica* and *R. equi*, both pathogen strains [13, 14]. Rifampicin is used for tuberculosis treatment and drug inactivation in *Mycobacterium* is driven by decomposition as in *Rhodococcus* and *Nocardia* species [14]. *N*-hydroxylation is an unusual reaction for

Table 4
HPLC product analysis of the 3HB6H reaction (see Section 3.3).

Substrate	Retention time	Product(s)	Retention time
3-hydroxybenzoate	19	2,5-dihydroxybenzoate	12.3
2,5-dihydroxybenzoate	11.7	–	12.3
3,5-dihydroxybenzoate	7.2	2,3,5-trihydroxybenzoate	4
		2,3,5,6-tetrahydroxybenzoate	2.7
2,3-dihydroxybenzoate	19.5	2,3,6-trihydroxybenzoate	4.1
3,4-dihydroxybenzoate	8.3	–	7.8
2,3,4-trihydroxybenzoate	8.6	2,3,4,6-tetrahydroxybenzoate	2.9
3-hydroxy-4-aminobenzoate	5.1	4-amino-2,5-dihydroxybenzoate	5.8
3-hydroxy-4-methylbenzoate	22.8	4-methyl-2,5-dihydroxybenzoate	17.5
3-hydroxy-4-methoxybenzoate	21.5	4-methoxy-2,5-dihydroxybenzoate	4.7

flavoprotein hydroxylases, usually performed by subclass B monooxygenases [42–47]. However, a hybrid kinetic mechanism between flavoprotein hydroxylases and subclass B monooxygenases has been reported for L-ornithine N5-oxygenase [46, 48]

Q0RW34 and Q0S9K8 are predicted to be a 3-(2-hydroxyphenyl) propionate hydroxylase and 6-hydroxynicotinate 3-monooxygenase, respectively. The first enzyme plays a role in lignin degradation [27], whereas the latter is involved in the metabolism of nicotinic acid in *P. fluorescence* T5 and *Pseudomonas putida* KT2400 [30, 31], performing decarboxylative hydroxylation of 6-hydroxynicotinic acid into 2,5-dihydroxypyridine.

Q0SJC8 most likely acts on an activated substrate, similarly to SibG [29, 49, 50], 2-aminobenzoylCoA monooxygenase/reductase (ACMR) and salicyl-CoA 5-hydroxylase. Interestingly, all the latter enzymes cluster in the same part of the tree (Fig. 2), suggesting that they might have a conserved mode of CoA-substrate recognition.

Q0SFK6 represents a clear mis-annotation in the *R. jostii* genome. From comparing several known 3HB6H amino acid sequences and gene clusters with the Q0SFK6 *Rhodococcus* DNA locus, we conclude that Q0SFK6 encodes for a 3HB6H which is involved in the gentisate degradation pathway. The organisation of the gene cluster is conserved in *C. glutamicum* and in *R. opacus* B4, and to a lesser extent in *Rhodococcus* NCIMB 12038 (Fig. 3). The presence of many regulatory elements or transposase-like elements surrounding most of the 3HB6H clusters could be viewed as an element of plasticity of this cluster, since gentisate formation could involve also salicylate 5-hydroxylase.

The enzymatic activity of Q0SKF6 was addressed with the recombinant protein. In agreement with the above proposition derived from sequence data, activity was found with 3-hydroxybenzoate and not with salicylate. Product analysis confirmed that Q0SKF6 encodes for 3HB6H and thus is mis-annotated as a salicylate hydroxylase.

Analytical gel filtration indicated that 3HB6H from *R. jostii* RHA1 is a homodimer. So far, a monomeric [51] or trimeric [34, 35, 52, 53] nature has been reported for 3HB6H enzymes. 3HB6H from *R. jostii* RHA1 has narrow substrate specificity. Besides the parent substrate, the enzyme accepts 3-hydroxybenzoate compounds with substituents in *ortho*- and *meta*-position. Importantly, it was established here for the first time that gentisate is a non-substrate effector of 3HB6H, stimulating FAD reduction and NADH consumption with production of hydrogen peroxide. Such behaviour of the aromatic product is also seen with the prototype of this flavoprotein subfamily, PHBH [28]. In case of 3HB6H, waste of NADH consumption will be negligible under physiological conditions, since gentisate dioxygenases convert gentisate very efficiently [54], preventing hydrogen peroxide production in the cell.

Three different microbial enzymes that produce gentisate have been reported: flavin-dependent salicyl-CoA 5-hydroxylase, Rieske (2Fe–2S) dependent salicylate 5-hydroxylase, and flavin-dependent 3HB6H. Salicyl-CoA 5-hydroxylase has been characterised in *Streptomyces* WA46 [49], while two-component Rieske type salicylate 5-hydroxylase has been studied in *Ralstonia* sp. U2 and *Polaromonas naphthalenivorans* CJ2 [21, 55]. Different 3HB6Hs have been described in Gram-positive [34, 35] and Gram-negative bacteria [51–53], and recently in *C. parapsilosis* [36].

Among *Rhodococcus* species, gentisate formation has been mostly related to salicylate 5-hydroxylase activity. Grund and colleagues measured salicyl-CoA 5-hydroxylase activity in *R. opacus* B4 cell extracts [56] and Di Gennaro and colleagues [57] described a gene cluster in *Rhodococcus* R7 containing a salicyl-CoA 5-hydroxylase gene. However, in both cases, no sequence or evidence at the enzyme level was reported. By using the *R. jostii* 3HB6H sequence as bait among the *Rhodococcus* genomes available, we found a putative 3HB6H in *R. opacus* B4 contained in a conserved 3-hydroxybenzoate/gentisate-degradation operon (Fig. 3). In contrast, with salicyl-CoA 5-hydroxylase (Q7X281) and salicylate 5-hydroxylase (Q3S4D3) as

baits, no *Rhodococcus* homologues were found. Recently, a 3HB6H was described in *Rhodococcus* sp. NCIMB 12038 [35]. 3HB6H from *R. jostii* RHA1 shares 93% amino acid sequence with 3HB6H from *Rhodococcus* sp. NCIMB 12038. To our best knowledge, these are the only *Rhodococcus* gentisate producing enzymes characterised thus far.

5. Conclusion

In conclusion, we have retrieved a pool of flavoprotein hydroxylases in *R. jostii* RHA1 that share conserved flavoprotein fingerprints but can act on diverse aromatic substrates. Furthermore, from multiple sequence alignments and phylogenetic analysis, a number of functional annotations have been resolved.

QOSFK6 is an example of a successful functional annotation. From biochemical analysis we obtained clear evidence that QOSFK6 was mis-annotated as a salicylate hydroxylase, an enzyme related to 3HB6H but with a different substrate specificity. 3HB6H is one of the few *para*-hydroxylating flavoprotein monooxygenases characterised. Recently, Hiromoto and coworkers [58] obtained the crystal structure of 3-hydroxybenzoate 4-hydroxylase (3HB4H) from *Comamonas testosteroni*. 3HB4H is using the same substrate as 3HB6H but performs an *ortho*-hydroxylation reaction. Comparison between structure and mechanism of 3HB4H and 3HB6H might help in understanding the striking regioselectivity of flavoprotein aromatic hydroxylases.

Supplementary data to this article can be found online at doi:10.1016/j.bbapap.2011.12.003.

Acknowledgements

We are grateful to Anette Riebel and Daniel Torres Pazmiño for In-Fusion PCR Cloning System optimisation, Laura de Hoon for experimental contributions and Adrië Westphal for technical assistance. This study was supported by the Integrated Biosynthesis Organic Synthesis (IBOS) project of the Netherlands Organization for Scientific Research (NWO).

References

- [1] M. Ahmad, J.N. Roberts, E.M. Hardiman, R. Singh, L.D. Eltis, T.D. Bugg, Identification of DypB from *Rhodococcus jostii* RHA1 as a lignin peroxidase, *Biochemistry* 50 (2011) 5096–5107.
- [2] M.J. Larkin, L.A. Kulakov, C.C.R. Allen, Biodegradation and *Rhodococcus*-masters of catabolic versatility, *Curr. Opin. Biotechnol.* 16 (2005) 282–290.
- [3] M.J. Larkin, L.A. Kulakov, C.C.R. Allen, Biodegradation by members of the genus *Rhodococcus*: biochemistry, physiology, and genetic adaptation, *Adv. Appl. Microbiol.* 59 (2006) 1–29.
- [4] L. Martínková, B. Uhnáková, M. Pátek, J. Nesvera, V. Kren, Biodegradation potential of the genus *Rhodococcus*, *Environ. Int.* 35 (2009) 162–177.
- [5] M.P. McLeod, R.L. Warren, W.W.L. Hsiao, N. Araki, M. Myhre, C. Fernandes, D. Miyazawa, W. Wong, A.L. Lillquist, D. Wang, M. Dosanjh, H. Hara, A. Petrescu, R.D. Morin, G. Yang, J.M. Stott, J.E. Schein, H. Shin, D. Smailus, A.S. Siddiqui, M.A. Marra, S.J.M. Jones, R. Holt, F.S.L. Brinkman, K. Miyauchi, M. Fukuda, J.E. Davies, W.W. Mohn, L.D. Eltis, The complete genome of *Rhodococcus* sp. RHA1 provides insights into a catabolic powerhouse, *Proc. Natl. Acad. Sci. U. S. A.* 103 (2006) 15582–15587.
- [6] W.J.H. van Berkel, N.M. Kamerbeek, M.W. Fraaije, Flavoprotein monooxygenases, a diverse class of oxidative biocatalysts, *J. Biotechnol.* 124 (2006) 670–689.
- [7] R. Hammann, H.J. Kutzner, Key enzymes for the degradation of benzoate, *m*- and *p*-hydroxybenzoate by some members of the order *Actinomycetales*, *J. Basic Microbiol.* 38 (1998) 207–220.
- [8] C.S. Harwood, R.E. Parales, The β -ketoadipate pathway and the biology of self-identity, *Annu. Rev. Microbiol.* 50 (1996) 553–590.
- [9] P.S. Phale, A. Basu, P.D. Majhi, J. Deveryshetty, C. Vamsee-Krishna, R. Shrivastava, Metabolic diversity in bacterial degradation of aromatic compounds, *OMICS* 11 (2007) 252–279.
- [10] P. Kallio, Z. Liu, P. Mantala, J. Niemi, M. Metsä-Ketela, Sequential action of two flavoenzymes, PgaE and PgaM, in angucycline biosynthesis: chemoenzymatic synthesis of gaudimycin C, *Chem. Biol.* 15 (2008) 157–166.
- [11] Y. Lindqvist, H. Koskineniemi, A. Jansson, T. Sandalova, R. Schnell, Z. Liu, P. Mäntylä, J. Niemi, G. Schneider, Structural basis for substrate recognition and specificity in aklavinone-11-hydroxylase from rhodomycin biosynthesis, *J. Mol. Biol.* 393 (2009) 966–977.
- [12] K.S. Ryan, A.R. Howard-Jones, M.J. Hamill, S.J. Elliott, C.T. Walsh, C.L. Drennan, Crystallographic trapping in the rebeccamycin biosynthetic enzyme RebC, *Proc. Natl. Acad. Sci. U. S. A.* 104 (2007) 15311–15316.
- [13] S.J. Andersen, S. Qian, B. Gowan, E.R. Dabbs, Monooxygenase-like sequence of a *Rhodococcus equi* gene conferring increased resistance to rifampin by inactivating this antibiotic, *Antimicrob. Agents Chemother.* 41 (1997) 218–221.
- [14] Y. Hoshino, S. Fujii, H. Shinonaga, K. Arai, F. Saito, T. Fukai, H. Satoh, Y. Miyazaki, J. Ishikawa, Monooxygenation of rifampicin catalyzed by the rox gene product of *Nocardia farcinica*: structure elucidation, gene identification and role in drug resistance, *J. Antibiot. (Tokyo)* 63 (2010) 23–28.
- [15] G. Volkers, G.J. Palm, M.S. Weiss, G.D. Wright, W. Hinrichs, Structural basis for a new tetracycline resistance mechanism relying on the TetX monooxygenase, *FEBS Lett.* 585 (2011) 1061–1066.
- [16] M.H. Eppink, H.A. Schreuder, W.J. van Berkel, Identification of a novel conserved sequence motif in flavoprotein hydroxylases with a putative dual function in FAD/NAD(P)H binding, *Protein Sci.* 6 (1997) 2454–2458.
- [17] R.K. Wierenga, P. Terpstra, W.G. Hol, Prediction of the occurrence of the ADP-binding $\beta\alpha\beta$ -fold in proteins, using an amino acid sequence fingerprint, *J. Mol. Biol.* 187 (1986) 101–107.
- [18] G. Eggink, H. Engel, G. Vriend, P. Terpstra, B. Witholt, Rubredoxin reductase of *Pseudomonas oleovorans*. Structural relationship to other flavoprotein oxidoreductases based on one NAD and two FAD fingerprints, *J. Mol. Biol.* 212 (1990) 135–142.
- [19] P. Macheroux, B. Kappes, S.E. Ealick, Flavogenomics – a genomic and structural view on flavin-dependent proteins, *FEBS J.* 278 (2011) 2625–2634.
- [20] S.L. Fuenmayor, M. Wild, A.L. Boyes, P.A. Williams, A gene cluster encoding steps in conversion of naphthalene to gentisate in *Pseudomonas* sp. strain U2, *J. Bacteriol.* 180 (1998) 2522–2530.
- [21] C.O. Jeon, M. Park, H.-S. Ro, W. Park, E.L. Madsen, The naphthalene catabolic (nag) genes of *Polaromonas naphthalenivorans* CJ2: evolutionary implications for two gene clusters and novel regulatory control, *Appl. Environ. Microbiol.* 72 (2006) 1086–1095.
- [22] J.D. Thompson, D.G. Higgins, T.J. Gibson, CLUSTAL W: improving the sensitivity of progressive multiple sequence alignment through sequence weighting, position-specific gap penalties and weight matrix choice, *Nucleic Acids Res.* 22 (1994) 4673–4680.
- [23] U.K. Laemmli, Cleavage of structural proteins during the assembly of the head of bacteriophage T4, *Nature* 227 (1970) 680–685.
- [24] R.A. Wijnands, J. van der Zee, J.W. Van Leeuwen, W.J. van Berkel, F. Müller, The importance of monopole-monopole and monopole-dipole interactions on the binding of NADPH and NADPH analogues to *p*-hydroxybenzoate hydroxylase from *Pseudomonas fluorescens*. Effects of pH and ionic strength, *Eur. J. Biochem.* 139 (1984) 637–644.
- [25] K.A. Johnson, R.S. Goody, The original Michaelis constant: translation of the 1913 Michaelis-Menten paper, *Biochemistry* 50 (2011) 8264–8269.
- [26] Y.J. Bollen, S.M. Nabuurs, W.J. van Berkel, C.P. van Mierlo, Last in, first out: the role of cofactor binding in flavodoxin folding, *J. Biol. Chem.* 280 (2005) 7836–7844.
- [27] J.A. Powell, J.A. Archer, Molecular characterisation of a *Rhodococcus* ohp operon, *Antonie Van Leeuwenhoek* 74 (1998) 175–188.
- [28] B. Entsch, W.J. van Berkel, Structure and mechanism of *para*-hydroxybenzoate hydroxylase, *FASEB J.* 9 (1995) 476–483.
- [29] T.W. Giessen, F.I. Kraas, M.A. Marahiel, A four-enzyme pathway for 3,5-dihydroxy-4-methylanthranilic acid formation and incorporation into the antitumor antibiotic sibiromycin, *Biochemistry* 50 (2011) 5680–5692.
- [30] J.I. Jimenez, A. Canales, J. Jimenez-Barbero, K. Ginalski, L. Rychlewski, J.L. Garcia, E. Diaz, Deciphering the genetic determinants for aerobic nicotinic acid degradation: the nic cluster from *Pseudomonas putida* KT2440, *Proc. Natl. Acad. Sci. U. S. A.* 105 (2008) 11329–11334.
- [31] H. Nakano, M. Wieser, B. Huh, T. Kawai, T. Yoshida, T. Yamane, T. Nagasawa, Purification, characterization and gene cloning of 6-hydroxynicotinate 3-monooxygenase from *Pseudomonas fluorescens* TN5, *Eur. J. Biochem.* 260 (1999) 120–126.
- [32] N.L. Huang, K. Itoh, M. Miyamoto, K. Suyama, H. Yamamoto, Chlorophenol hydroxylase activity encoded by TfdB from 2,4-dichlorophenoxyacetic acid (2,4-D)-degrading *Bradyrhizobium* sp. strain RD5-C2, *Biosci. Biotechnol. Biochem.* 71 (2007) 1691–1696.
- [33] X.-H. Shen, C.-Y. Jiang, Y. Huang, Z.-P. Liu, S.-J. Liu, Functional identification of novel genes involved in the glutathione-independent gentisate pathway in *Corynebacterium glutamicum*, *Appl. Environ. Microbiol.* 71 (2005) 3442–3452.
- [34] Y.F. Yang, J.J. Zhang, S.H. Wang, N.Y. Zhou, Purification and characterization of the ncg12923-encoded 3-hydroxybenzoate 6-hydroxylase from *Corynebacterium glutamicum*, *J. Basic Microbiol.* 50 (2010) 599–604.
- [35] T.T. Liu, Y. Xu, H. Liu, S. Luo, Y.J. Yin, S.J. Liu, N.Y. Zhou, Functional characterization of a gene cluster involved in gentisate catabolism in *Rhodococcus* sp. strain NCIMB 12038, *Appl. Microbiol. Biotechnol.* 90 (2010) 671–678.
- [36] Z. Holesova, M. Jakubkova, I. Zavadikova, I. Zeman, L. Tomaska, J. Nosek, Gentisate and 3-oxoadipate pathways in the yeast *Candida parapsilosis*: Identification and functional analysis of the genes coding for 3-hydroxybenzoate 6-hydroxylase and 4-hydroxybenzoate 1-hydroxylase, *Microbiology* 157 (2011) 2152–2163.
- [37] M.H. Eppink, S.A. Boeren, J. Vervoort, W.J. van Berkel, Purification and properties of 4-hydroxybenzoate 1-hydroxylase (decarboxylating), a novel flavin adenine dinucleotide-dependent monooxygenase from *Candida parapsilosis* CBS604, *J. Bacteriol.* 179 (1997) 6680–6687.
- [38] P.J. Steennis, M.M. Cordes, J.H. Hilken, F. Muller, On the interaction of *para*-hydroxybenzoate hydroxylase from *Pseudomonas fluorescens* with halogen ions, *FEBS Lett.* 36 (1973) 177–180.
- [39] W.J. van Berkel, W.J. van den Tweel, Purification and characterisation of 3-hydroxyphenylacetate 6-hydroxylase: a novel FAD-dependent monooxygenase from a *Flavobacterium* species, *Eur. J. Biochem.* 201 (1991) 585–592.

- [40] W.J. van Berkel, F. Müller, Flavin-dependent monooxygenase with special references to *p*-hydroxybenzoate hydroxylase, in: B. Raton (Ed.), Chemistry and biochemistry of flavoenzymes, 2, CRC Press, 1991, pp. 1–29.
- [41] C. Szolkowy, L.D. Eltis, N.C. Bruce, G. Grogan, Insights into sequence–activity relationships amongst Baeyer–Villiger monooxygenases as revealed by the intragenomic complement of enzymes from *Rhodococcus jostii* RHA1, *Chembiochem* 10 (2009) 1208–1217.
- [42] D.E. Torres Pazmiño, H.M. Dudek, M.W. Fraaije, Baeyer–Villiger monooxygenases: recent advances and future challenges, *Curr. Opin. Chem. Biol.* 14 (2010) 138–144.
- [43] S.W. Chocklett, P. Sobrado, *Aspergillus fumigatus* SidA is a highly specific ornithine hydroxylase with bound flavin cofactor, *Biochemistry* 49 (2010) 6777–6783.
- [44] L. Ge, S.Y. Seah, Heterologous expression, purification, and characterization of an L-ornithine N(5)-hydroxylase involved in pyoverdine siderophore biosynthesis in *Pseudomonas aeruginosa*, *J. Bacteriol.* 188 (2006) 7205–7210.
- [45] J.A. Mayfield, R.E. Frederick, B.R. Streit, T.A. Wenczewicz, D.P. Ballou, J.L. DuBois, Comprehensive spectroscopic, steady state, and transient kinetic studies of a representative siderophore-associated flavin monooxygenase, *J. Biol. Chem.* 285 (2010) 30375–30388.
- [46] K.M. Meneely, E.W. Barr, J.M. Bollinger, A.L. Lamb, Kinetic mechanism of ornithine hydroxylase (PvdA) from *Pseudomonas aeruginosa*: substrate triggering of O₂ addition but not flavin reduction, *Biochemistry* 48 (2009) 4371–4376.
- [47] K.M. Meneely, A.L. Lamb, Biochemical characterization of a flavin adenine dinucleotide-dependent monooxygenase, ornithine hydroxylase from *Pseudomonas aeruginosa*, suggests a novel reaction mechanism, *Biochemistry* 46 (2007) 11930–11937.
- [48] J. Olucha, A.L. Lamb, Mechanistic and structural studies of the *N*-hydroxylating flavoprotein monooxygenases, *Bioorg. Chem.* 39 (2011) 171–177.
- [49] D. Ishiyama, D. Vujaklija, J. Davies, Novel pathway of salicylate degradation by *Streptomyces* sp. strain WA46, *Appl. Environ. Microbiol.* 70 (2004) 1297–1306.
- [50] K. Schuhle, M. Jahn, S. Ghisla, G. Fuchs, Two similar gene clusters coding for enzymes of a new type of aerobic 2-aminobenzoate (anthranilate) metabolism in the bacterium *Azoarcus evansii*, *J. Bacteriol.* 183 (2001) 5268–5278.
- [51] M. Suarez, E. Ferrer, A. Garrido-Pertierra, M. Martin, Purification and characterization of the 3-hydroxybenzoate-6-hydroxylase from *Klebsiella pneumoniae*, *FEMS Microbiol. Lett.* 126 (1995) 283–290.
- [52] X. Gao, C.L. Tan, C.C. Yeo, C.L. Poh, Molecular and biochemical characterization of the xlnD-encoded 3-hydroxybenzoate 6-hydroxylase involved in the degradation of 2,5-xyleneol via the gentisate pathway in *Pseudomonas alcaligenes* NCIMB 9867, *J. Bacteriol.* 187 (2005) 7696–7702.
- [53] M. Park, Y. Jeon, H.H. Jang, H.-S. Ro, W. Park, E.L. Madsen, C.O. Jeon, Molecular and biochemical characterization of 3-hydroxybenzoate 6-hydroxylase from *Polaromonas naphthalenivorans* CJ2, *Appl. Environ. Microbiol.* 73 (2007) 5146–5152.
- [54] M.A. Adams, V.K. Singh, B.O. Keller, Z. Jia, Structural and biochemical characterization of gentisate 1,2-dioxygenase from *Escherichia coli* O157:H7, *Mol. Microbiol.* 61 (2006) 1469–1484.
- [55] N.-Y. Zhou, J. Al-Dulayymi, M.S. Baird, P.A. Williams, Salicylate 5-hydroxylase from *Ralstonia* sp. strain U2: a monooxygenase with close relationships to and shared electron transport proteins with naphthalene dioxygenase, *J. Bacteriol.* 184 (2002) 1547–1555.
- [56] E. Grund, B. Denecke, R. Eichenlaub, Naphthalene degradation via salicylate and gentisate by *Rhodococcus* sp. strain B4, *Appl. Environ. Microbiol.* 58 (1992) 1874–1877.
- [57] P. Di Gennaro, P. Terreni, G. Masi, S. Botti, F. De Ferra, G. Bestetti, Identification and characterization of genes involved in naphthalene degradation in *Rhodococcus opacus* R7, *Appl. Microbiol. Biotechnol.* 87 (2010) 297–308.
- [58] T. Hiromoto, S. Fujiwara, K. Hosokawa, H. Yamaguchi, Crystal structure of 3-hydroxybenzoate hydroxylase from *Comamonas testosteroni* has a large tunnel for substrate and oxygen access to the active site, *J. Mol. Biol.* 364 (2006) 878–896.